Phys. Lett. B 858 (2024) 139032

Contents lists available at ScienceDirect

Physics Letters B

journal homepage: www.elsevier.com/locate/physletb

Letter

Measurement of J/ψ and $\psi(2S)$ production in $p+p$ and $p+d$ interactions at 120 GeV

SeaQuest Collaboration

C.H. Leung [a,*,1], K. Nagai [b,c,d,2], K. Nakano [b,e,f], D. Nawarathne [g], J. Dove [a], S. Prasad [a,h], N. Wuerfel [i], C.A. Aidala [i,d], J. Arrington [h,3], C. Ayuso [i], C.L. Barker [j], C.N. Brown [k], W.C. Chang [c], A. Chen [a,c,i], D.C. Christian [k], B.P. Dannowitz [a], M. Daugherity [j], L. El Fassi [l,m], D.F. Geesaman [h], R. Gilman [m], Y. Goto [e], R. Guo [n], T.J. Hague [j,3], R.J. Holt [h,4], M.F. Hossain [g], D. Isenhower [j], E. Kinney [o], A. Klein [d], D.W. Kleinjan [d], Y. Kudo [p], P.-J. Lin [o,c,5], K. Liu [d], M.X. Liu [d], W. Lorenzon [i], R.E. McClellan [a,6], P.L. McGaughey [d], M.M. Medeiros [h], Y. Miyachi [p], S. Miyasaka [b], D.H. Morton [i], K. Nakahara [q,7], S. Nara [p], S.F. Pate [g], J.C. Peng [a], A. Pun [g], B.J. Ramson [i,k], P.E. Reimer [h], J.G. Rubin [i,h], F. Sanftl [b], S. Sawada [r], T. Sawada [i,8], M.B.C. Scott [i,h,9], T.-A. Shibata [b,e,10], A.S. Tadepalli [m,1], M. Teo [a], R.S. Towell [j], S. Uemura [d,11], S.G. Wang [c,n,12], A.B. Wickes [d], J. Wu [k], Z.H. Ye [h,13]

[a] Department of Physics, University of Illinois at Urbana-Champaign, Urbana, IL 61801, USA
[b] Department of Physics, Tokyo Institute of Technology, Meguro-ku, Tokyo 152-8550, Japan
[c] Institute of Physics, Academia Sinica, Taipei 11529, Taiwan
[d] Physics Division, Los Alamos National Laboratory, Los Alamos, NM 87545, USA
[e] RIKEN Nishina Center for Accelerator-Based Science, Wako, Saitama 351-0198, Japan
[f] University of Virginia, Charlottesville, VA 22904, USA
[g] Department of Physics, New Mexico State University, Las Cruces, NM 88003, USA
[h] Physics Division, Argonne National Laboratory, Lemont, IL 60439, USA
[i] Randall Laboratory of Physics, University of Michigan, Ann Arbor, MI 48109, USA
[j] Department of Engineering and Physics, Abilene Christian University, Abilene, TX 79699, USA
[k] Fermi National Accelerator Laboratory, Batavia, IL 60510, USA
[l] Department of Physics and Astronomy, Mississippi State University, Mississippi State, MS 39762, USA
[m] Department of Physics and Astronomy, Rutgers, The State University of New Jersey, Piscataway, NJ 08854, USA

* Corresponding author.
E-mail addresses: chleung@illinois.edu, cleung@jlab.org (C.H. Leung).
[1] Present address: Thomas Jefferson National Accelerator Facility, Newport News, Virginia 23606, USA.
[2] Present address: Duke University, Durham, North Carolina 27710, USA.
[3] Present address: Lawrence Berkeley National Laboratory, Berkeley, California, 94720, USA.
[4] Present address: Kellogg Radiation Laboratory, California Institute of Technology, Pasadena, California 91125, USA.
[5] Present address: Center for High Energy and High Field Physics and Department of Physics, National Central University, Taoyuan City 320317, Taiwan.
[6] Present address: Pensacola State College, Pensacola, FL 32504, USA.
[7] Present address: Stanford Linear Accelerator Center, Menlo Park, CA 94025, USA.
[8] Present address: Institute for Cosmic Ray Research, KAGRA Observatory, The University of Tokyo, Hida, Gifu 506-1205, Japan.
[9] Present address: George Washington University, Washington, DC 20052, USA.
[10] Present address: Nihon University, College of Science and Technology, Chiyoda-ku, Tokyo 101-8308, Japan.
[11] Present address: Fermi National Accelerator Laboratory, Batavia, Illinois 60510, USA.
[12] Present address: APS, Argonne National Laboratory, Lemont, Illinois 60439, USA.
[13] Present address: Department of Physics, Tsinghua University, Beijing 100084, China.

https://doi.org/10.1016/j.physletb.2024.139032
Received 21 June 2024; Received in revised form 15 September 2024; Accepted 16 September 2024
Available online 18 September 2024

[n] Department of Physics, National Kaohsiung Normal University, Kaohsiung City 80201, Taiwan
[o] Department of Physics, University of Colorado, Boulder, CO 80309, USA
[p] Department of Physics, Yamagata University, Yamagata City, Yamagata 990-8560, Japan
[q] Department of Physics, University of Maryland, College Park, MD 20742, USA
[r] Institute of Particle and Nuclear Studies, KEK, High Energy Accelerator Research Organization, Tsukuba, Ibaraki 305-0801, Japan

ARTICLE INFO

Editor: H. Gao

ABSTRACT

We report the $p+p$ and $p+d$ differential cross sections measured in the SeaQuest experiment for J/ψ and $\psi(2S)$ production at 120 GeV beam energy covering the forward x-Feynman (x_F) range of $0.5 < x_F < 0.9$. The measured cross sections are in good agreement with theoretical calculations based on the nonrelativistic QCD (NRQCD) using the long-distance matrix elements deduced from a recent global analysis of proton- and pion-induced charmonium production data. The $\sigma_{\psi(2S)}/\sigma_{J/\psi}$ cross section ratios are found to increase as x_F increases, indicating that the $q\bar{q}$ annihilation process has larger contributions in the $\psi(2S)$ production than the J/ψ production. The $\sigma_{pd}/2\sigma_{pp}$ cross section ratios are observed to be significantly different for the Drell-Yan process and J/ψ production, reflecting their different production mechanisms. We find that the $\sigma_{pd}/2\sigma_{pp}$ ratios for J/ψ production at the forward x_F region are sensitive to the $\bar{d}/\bar{u}$ flavor asymmetry of the proton sea, analogous to the Drell-Yan process. The transverse momentum (p_T) distributions for J/ψ and $\psi(2S)$ production are also presented and compared with data collected at higher center-of-mass energies.

The SeaQuest experiment at Fermilab measures high-mass dimuons produced in the interaction of a 120 GeV proton beam with various targets including liquid hydrogen, liquid deuterium, and nuclear targets [1]. Dimuons originating from the Drell-Yan process [2] and from the decay of charmonium states (J/ψ and $\psi(2S)$) were collected simultaneously. Results from SeaQuest on the $\sigma_{pd}/2\sigma_{pp}$ Drell-Yan cross section ratio, which is sensitive to the $\bar{d}/\bar{u}$ flavor asymmetry in the proton, were reported recently [3,4]. In this paper, we present results from SeaQuest on the J/ψ and $\psi(2S)$ charmonium production in $p+p$ and $p+d$ interactions.

Unlike the Drell-Yan process which primarily involves the quark-antiquark annihilation through the electromagnetic interaction, charmonium production proceeds via the strong interaction containing both the quark-antiquark annihilation and the gluon-gluon fusion processes. The simultaneous measurement of these two very different processes provides complementary information on the partonic structures of the nucleon. In particular, the $\sigma_{pd}/2\sigma_{pp}$ ratio for charmonium production is expected to be sensitive to the ratio of the gluon distributions in the proton and neutron, as well as the $\bar{d}/\bar{u}$ ratio in the proton [5].

If quark-antiquark annihilation is an important subprocess for charmonium production, then the $\sigma_{pd}/2\sigma_{pp}$ ratio would provide an independent measurement of the $\bar{d}/\bar{u}$ flavor asymmetry in the proton [5], analogous to the Drell-Yan process. On the other hand, the gluon-gluon fusion subprocess would allow the $\sigma_{pd}/2\sigma_{pp}$ ratio to probe the relative gluon content in the proton and neutron, providing a test of the charge symmetry (CS) at the partonic level [6]. The CS operation interchanges the up and down quarks, and it also interchanges the proton and the neutron. Since the gluon is an iso-scalar particle, CS requires that the gluon distributions in the proton and neutron are identical. Violation of CS is predicted at both the hadronic [7,8] and the partonic [9] levels. A measurement of the gluon contents of the proton and neutron could test CS at the partonic level [6,10,11]. It is also interesting to compare the production mechanisms for J/ψ versus $\psi(2S)$.

While proton-induced charmonium production is often dominated by the gluon-gluon fusion process [12], the quark-antiquark annihilation process could also contribute significantly. The relative importance of these two processes depends on the beam energy and on the x-Feynman (x_F) (see Eq. (1)) of the charmonium [5], and can be calculated using various production models: color evaporation model (CEM) [13–15], color singlet model (CSM) [16], and nonrelativistic QCD (NRQCD) [17]. These various models predict different relative importance of the different subprocesses [18]. In this paper, we mainly focus on the comparison with NRQCD, with the comparison with CEM shown in the Supplemental Material.

The NA51 collaboration reported a measurement of the $p+p$ and $p+d$ cross sections for charmonium production at 450 GeV at a single value of $x_F \approx 0$ [19]. The SeaQuest measurement covers the broader kinematic range of $0.5 < x_F < 0.9$ at the lower beam energy of 120 GeV. These two measurements can provide complementary information.

The SeaQuest experiment was performed using the 120 GeV proton beam from the Fermilab Main Injector. The SeaQuest dimuon spectrometer was designed for detecting high-mass dimuon pairs produced in the interaction of a proton with various targets. Details of the SeaQuest spectrometer can be found elsewhere [1,3,4]. A primary proton beam containing up to 6×10^{12} protons in a 4-second long beam spill every minute was incident upon one of three identical 50.8 cm long cylindrical stainless steel target flasks or solid nuclear targets. The targets alternated between liquid hydrogen, liquid deuterium, solid nuclear targets, and the empty flask target. A Cherenkov counter was placed in the beam to record the instantaneous proton intensity for each 1-ns long RF bucket at a 53 MHz repetition rate.

The SeaQuest spectrometer consists of two dipole magnets and four detector stations equipped with hodoscopes and tracking chambers. A solid iron magnet downstream of the target focuses the dimuons and also serves as a beam-dump and a hadron absorber. An open magnet further downstream measures the muon momentum. The dimuon trigger requires a quadruple hodoscope coincidence with a pattern consistent with a muon pair originating from the target. Various diagnostic triggers are also implemented. In particular, the "single-muon" trigger is used to evaluate the accidental dimuon background, and the "random" trigger samples the detector response throughout the data-taking periods.

The SeaQuest data are separated into two sets, each containing roughly half of the total data sample. The first part includes data taken between June 2014 and July 2015, and the second part covers the remaining period up to July 2017. Results on the analysis of the Drell-Yan events from the first data set have already been reported [3,4]. In this paper, we have analyzed the full SeaQuest data sets. Since the trigger conditions and the detector configuration for the two data sets are not identical, the analysis was performed separately for each data set. Results obtained from the two data sets are first compared to verify their consistency, and then combined for the final results.

Details of the data analysis procedure can be found in Refs. [3,4]. Candidate muon tracks reconstructed in the drift chambers are extrapolated to the target region. Only dimuon events consistent with originating from the target are selected. The target position is then used to refine the parameters of each muon pair. The resulting RMS mass resolution for J/ψ is ≈200 MeV, dominated by the finite target length and the multiple scattering of muons in the iron magnet.

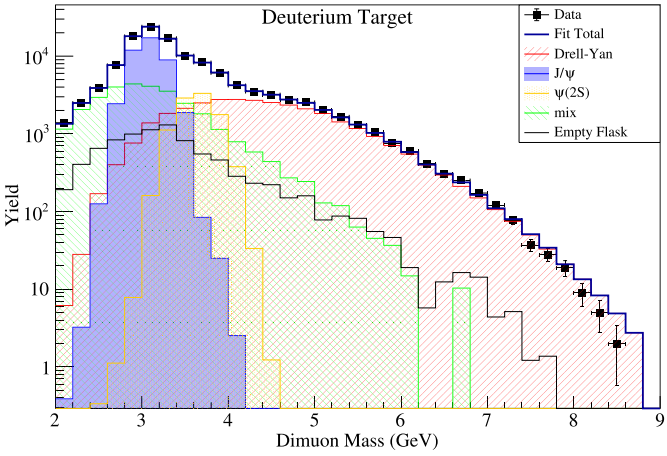

Fig. 1. Dimuon mass distribution for events collected on a liquid deuterium target for the second data set. The data points (solid squares) are compared with a fit (solid blue line) consisting of various components (see text).

Fig. 1 shows the dimuon mass spectrum for $p+d$ data collected in the second data set. A comparison with the mass spectrum obtained for the first data set, reported in Ref. [4], shows good agreement with some small differences attributed to the minor changes in trigger conditions and spectrometer settings.

To extract the yields of J/ψ and $\psi(2S)$, the dimuon mass spectrum is fitted by including several components. First, data collected with the empty target flask are analyzed to determine the background originating from sources other than the liquid. Second, a GEANT4 [24–26] based Monte Carlo (MC) simulation is performed to obtain the expected line shapes of the J/ψ and $\psi(2S)$ resonances. The MC dimuon events are then embedded with additional hits in the detectors using data collected with the "random" trigger, which randomly samples the spectrometer response to background hits. This procedure accounts for the spectrometer response to background hits. Third, dimuons from the Drell-Yan process are simulated using a next-to-leading order calculation [27] with the CT14 parton distribution functions (PDFs) [28], as described in an earlier publication [4]. The embedding procedure is also applied to the Drell-Yan MC data. Finally, the accidental dimuon background, caused by two independent interactions within the same RF bucket, is simulated by forming a random combination of data collected with the "single-muon" trigger, as discussed in detail in Ref. [4], labeled as "mix" in Fig. 1. Other mixing methods [29] have also been studied and included in the systematic uncertainties. These embedded MC events are then analyzed by applying cuts identical to those for the real data.

A fit to the $p+d$ dimuon data, allowing the normalizations of the various components except the empty flask data to vary, is shown in Fig. 1. The empty flask data are normalized according to their relative luminosity. The data are well described as the sum of various components. The adequacy of this approach is further validated by the excellent agreement between this method [4] and an independent intensity-extrapolation method [3] for the extracted $\sigma_{pd}/2\sigma_{pp}$ Drell-Yan cross section ratios.

To obtain the charmonium differential cross sections, the data were split into bins of x_F and p_T and the dimuon mass spectrum for each bin is fitted with the procedure described earlier to extract the J/ψ and $\psi(2S)$ yields. We note the following definition of x_F [3]:

$$x_F = \frac{2p_L}{\sqrt{s}\left(1 - M^2/s\right)}, \tag{1}$$

where p_L is the longitudinal momentum of the dimuon in the hadron-hadron center of mass frame. M and $\sqrt{s}$ are the dimuon mass and the hadron-hadron total energy, respectively. The charmonium production cross section is obtained as

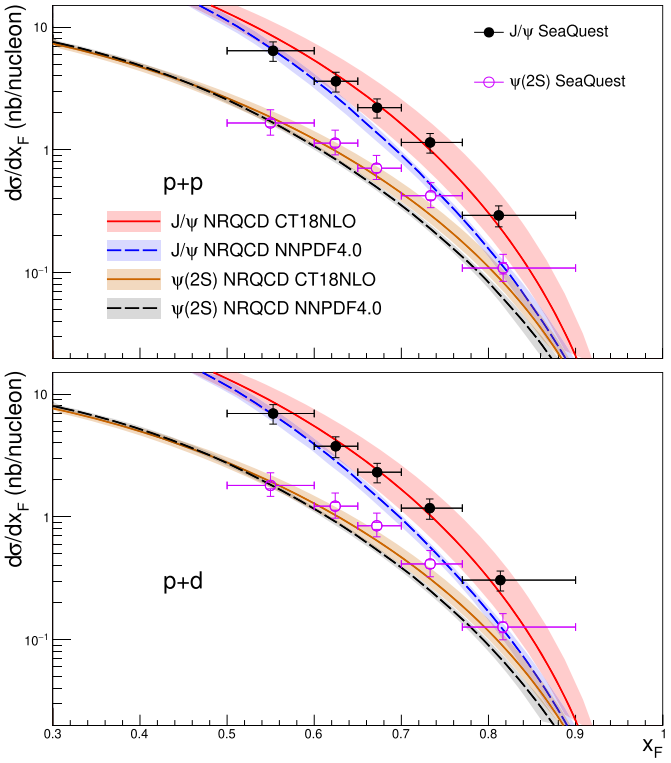

Fig. 2. The differential cross section per nucleon $d\sigma/dx_F$ for J/ψ and $\psi(2S)$ production in $p+p$ and $p+d$ interactions at 120 GeV, integrated over p_T. The error bars represent the total uncertainties. The curves correspond to NRQCD calculation [20] using the LDMEs obtained in [21] and the nucleon PDFs from CT18 [22] and NNPDF4.0 [23]. The error bands indicate 68% confidence level from the PDFs.

$$d\sigma = \frac{dY}{B \cdot \mathrm{Acc} \cdot \mathrm{Eff} \cdot \mathrm{Lum}}, \tag{2}$$

where the yield dY is the number of J/ψ or $\psi(2S)$ events for each x_F or p_T bin, Acc the spectrometer acceptance, Eff the efficiency for analysis cuts, Lum the effective luminosity including the data-acquisition deadtime, and B the branching ratio for decaying into a muon pair. We use $B\left(J/\psi \to \mu^+\mu^-\right) = (5.961 \pm 0.033)\,\%$ and $B\left(\psi(2S) \to \mu^+\mu^-\right) = (8.0 \pm 0.6) \times 10^{-3}$ [30].

The x_F dependence of the J/ψ and $\psi(2S)$ production cross sections in $p+p$ and $p+d$ collisions is shown in Fig. 2 and listed in Table 1. In this and the subsequent figures, the horizontal error bars represent the bin width, and the data points are positioned on the ordinate at the mean value for the events in the bin. The $d\sigma/dx_F$ differential cross sections are obtained with an acceptance calculation using a p_T distribution which best fits the data. The systematic uncertainties include an overall normalization uncertainty, common to both $p+p$ and $p+d$ cross sections. Other uncertainties which are largely independent of data set are the relative normalization of the flask data, the event mixing procedure ($\approx 7.2\%$), the trigger efficiency ($\approx 11\%$), reconstruction efficiency ($\approx 15\%$) and the trigger roadset dependence ($\approx 2\%$). A second set of uncertainties correlated between data sets are the J/ψ and $\psi(2S)$ polarization ($\approx 5.5\%$) and the uncertainty in the beam normalization ($\approx 10\%$). More discussion on the systematic uncertainties can be found in Ref. [35].

The $d\sigma/dx_F$ distributions of charmonium production are compared with theoretical calculations in Fig. 2. The calculations were performed using the non-relativistic QCD (NRQCD) [17,36] approach, which is based on the factorization of the heavy-quark $Q\bar{Q}$ pair production and its subsequent hadronization. The $Q\bar{Q}$ production includes the subprocesses of gluon-gluon fusion, quark-antiquark annihilation, and quark-gluon interaction. The hadronizations into quarkonium bound states are

Table 1
The differential cross sections per nucleon, $d\sigma/dx_F$ (in nb), for J/ψ and $\psi(2S)$ production in $p+p$ and $p+d$ collisions at 120 GeV for different x_F bins. The statistical uncertainties followed by systematic uncertainties are also shown.

$p+p$				$p+d$			
$\langle x_F\rangle_{J/\psi}$	$d\sigma/dx_F\|_{J/\psi}$	$\langle x_F\rangle_{\psi(2S)}$	$d\sigma/dx_F\|_{\psi(2S)}$	$\langle x_F\rangle_{J/\psi}$	$d\sigma/dx_F\|_{J/\psi}$	$\langle x_F\rangle_{\psi(2S)}$	$d\sigma/dx_F\|_{\psi(2S)}$
0.553	$6.411 \pm 0.246 \pm 1.130$	0.550	$1.654 \pm 0.112^{+0.451}_{-0.319}$	0.553	$6.944 \pm 0.275 \pm 1.224$	0.550	$1.802 \pm 0.112^{+0.468}_{-0.315}$
0.625	$3.618 \pm 0.145 \pm 0.647$	0.624	$1.134 \pm 0.079^{+0.302}_{-0.209}$	0.625	$3.758 \pm 0.166 \pm 0.706$	0.624	$1.222 \pm 0.088^{+0.329}_{-0.230}$
0.672	$2.204 \pm 0.082 \pm 0.383$	0.671	$0.709 \pm 0.055^{+0.184}_{-0.124}$	0.672	$2.309 \pm 0.087 \pm 0.408$	0.672	$0.846 \pm 0.055^{+0.220}_{-0.148}$
0.733	$1.149 \pm 0.037 \pm 0.205$	0.734	$0.423 \pm 0.031^{+0.113}_{-0.079}$	0.733	$1.177 \pm 0.039 \pm 0.217$	0.733	$0.413 \pm 0.032^{+0.114}_{-0.082}$
0.812	$0.293 \pm 0.011 \pm 0.056$	0.817	$0.109 \pm 0.012^{+0.030}_{-0.021}$	0.814	$0.305 \pm 0.013 \pm 0.055$	0.817	$0.127 \pm 0.013^{+0.034}_{-0.024}$

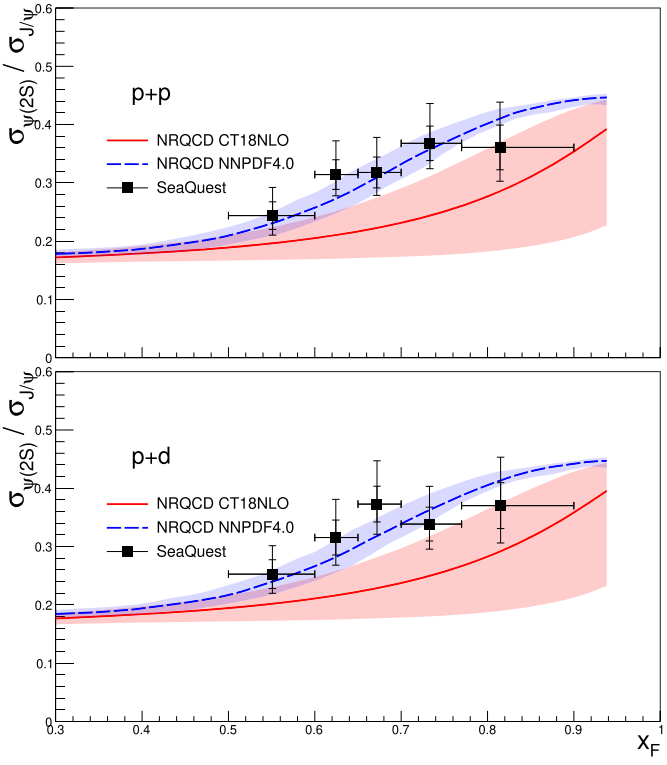

Fig. 3. The ratio of $\sigma_{\psi(2S)}/\sigma_{J/\psi}$ in $p+p$ and $p+d$ interactions at 120 GeV. The inner (outer) error bars represent the statistical (total) uncertainties. The curves correspond to NRQCD calculation using CT18 and NNPDF4.0. The error bands indicate 68% confidence level from the PDFs.

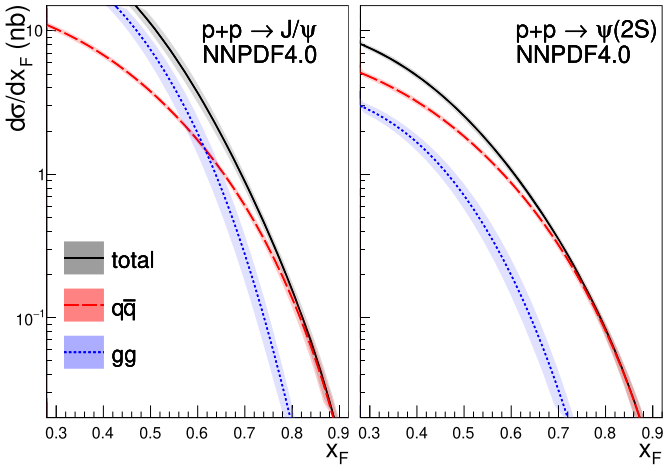

Fig. 4. The individual contribution from the $q\bar{q}$ (red dash) and gg (blue dotted) process to the production of J/ψ (left) and $\psi(2S)$ (right) calculated in NRQCD using NNPDF4.0 PDFs.

described by a set of long-distance matrix elements (LDMEs), assumed to be universal and fixed by the experimental data [20,36]. The LDMEs are taken from a recent global fit to fixed-target proton and pion induced J/ψ and $\psi(2S)$ production data performed with the SMRS pion and CT14 proton PDFs at charm mass $m_c = 1.5$ GeV in Ref. [21], which give the best overall χ^2 in their analysis. The estimated J/ψ cross section also includes the feed-down from hadronic decays of $\psi(2S)$ and radiative decays of the three χ_{cJ} states as described in Ref. [21]. Fig. 2 shows that the $d\sigma/dx_F$ data for $p+p$ and $p+d$ are very well described by the NRQCD calculation [20,36] using CT18 [22], including the overall normalization, which is fixed by the LDMEs. The extracted cross sections are also compared to the color evaporation model (CEM) [37–41] in Fig. S1. In the CEM framework, the hadronization probability is independent of the underlying sub-process, and it is typically obtained from fitting to data. As shown in Fig. S1 of the Supplemental Material, the measured J/ψ x_F distributions are also in good agreement with CEM calculations, but the CEM calculations tend to underestimate the $\psi(2S)$ cross section at large x_F.

The ratio of $\sigma_{\psi(2S)}/\sigma_{J/\psi}$ as a function of x_F is shown in Fig. 3. The measured ratio is found to increase as x_F increases, suggesting a broader x_F distribution for $\psi(2S)$ production than for J/ψ production. This behavior is well described by the NRQCD calculations as shown in Fig. 3. Since the valence quark in the proton has a much broader x distribution than the gluon, one expects the $q\bar{q}$ annihilation process would give a broader x_F distribution than the gluon-gluon fusion process. Therefore, the broader x_F distribution for $\psi(2S)$ production is attributed to the increasing importance of the $q\bar{q}$ annihilation process for $\psi(2S)$ production. This implies that the $\psi(2S)$ production is more analogous to the Drell-Yan process, which is dominated by the $q\bar{q}$ annihilation process. Fig. 4 shows the individual contribution from the $q\bar{q}$ annihilation and gluon fusion processes to the J/ψ and $\psi(2S)$ production in $p+p$ collision calculated in NRQCD using NNPDF4.0 PDFs. At $x_F \leq 0.6$, the gluon fusion process is more important than $q\bar{q}$ annihilation for J/ψ production. In contrast, the $\psi(2S)$ production is dominated by the $q\bar{q}$ annihilation process for the entire x_F range. Similar behavior was also observed for pion-induced J/ψ and $\psi(2S)$ production data [42].

It should be noted that the relative importance of these subprocesses remains uncertain and depends on the production model used [18]. Unlike NRQCD, the fragmentation probability in CEM is independent of the underlying sub-process, and only depends on the final charmonium state. Hence, CEM would suggest the x_F distribution to be identical for J/ψ and $\psi(2S)$, except for the relative fraction of $\psi(2S)$ production. Therefore CEM would predict the $\sigma_{\psi(2S)}/\sigma_{J/\psi}$ ratio to be independent of x_F, which qualitatively disagrees with the data shown in Fig. 3.

The p_T dependence of the J/ψ and $\psi(2S)$ cross sections is shown in Fig. 5 and listed in Table 2 for $p+p$ and $p+d$. The $d\sigma/dp_T^2$ differential cross sections are obtained by using the x_F distribution obtained from NRQCD to evaluate the spectrometer acceptance for J/ψ and $\psi(2S)$. These p_T distributions are fitted with the Kaplan parameter-

Table 2
The differential cross sections per nucleon, $d\sigma/dp_T^2$ (in nb GeV^{-2}), for charmonium production in $p+p$ and $p+d$ collisions at 120 GeV for different p_T bins. The statistical uncertainties followed by systematic uncertainties are also shown.

$p+p$				$p+d$			
$\langle p_T\rangle_{J/\psi}$	$d\sigma/dp_T^2\big\|_{J/\psi}$	$\langle p_T\rangle_{\psi(2S)}$	$d\sigma/dp_T^2\big\|_{\psi(2S)}$	$\langle p_T\rangle_{J/\psi}$	$d\sigma/dp_T^2\big\|_{J/\psi}$	$\langle p_T\rangle_{\psi(2S)}$	$d\sigma/dp_T^2\big\|_{\psi(2S)}$
0.195	$3.570 \pm 0.134 \pm 0.605$	0.195	$0.957 \pm 0.059^{+0.200}_{-0.160}$	0.193	$3.789 \pm 0.137 \pm 0.634$	0.194	$1.017 \pm 0.055^{+0.211}_{-0.169}$
0.376	$3.045 \pm 0.114 \pm 0.519$	0.376	$0.827 \pm 0.043^{+0.181}_{-0.149}$	0.376	$3.119 \pm 0.115 \pm 0.558$	0.377	$0.864 \pm 0.046^{+0.185}_{-0.150}$
0.550	$2.196 \pm 0.070 \pm 0.392$	0.551	$0.669 \pm 0.031^{+0.145}_{-0.119}$	0.550	$2.251 \pm 0.071 \pm 0.421$	0.553	$0.645 \pm 0.030^{+0.137}_{-0.111}$
0.761	$1.373 \pm 0.052 \pm 0.261$	0.764	$0.367 \pm 0.023^{+0.102}_{-0.091}$	0.761	$1.337 \pm 0.056 \pm 0.277$	0.764	$0.355 \pm 0.025^{+0.109}_{-0.099}$
1.095	$0.473 \pm 0.021 \pm 0.086$	1.106	$0.122 \pm 0.011^{+0.035}_{-0.031}$	1.098	$0.506 \pm 0.022 \pm 0.096$	1.111	$0.108 \pm 0.012^{+0.037}_{-0.035}$
$\langle p_T^2\rangle = 0.714 \pm 0.021 \pm 0.040$		$\langle p_T^2\rangle = 0.714 \pm 0.036 \pm 0.068$		$\langle p_T^2\rangle = 0.717 \pm 0.022 \pm 0.046$		$\langle p_T^2\rangle = 0.663 \pm 0.035 \pm 0.067$	

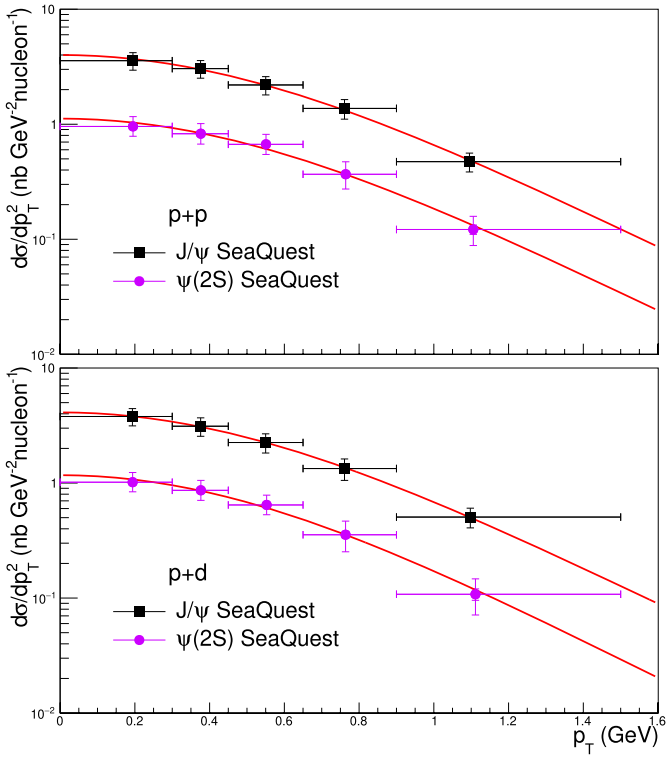

Fig. 5. The differential cross section per nucleon $d\sigma/dp_T^2$, integrated over $0.5 < x_F < 0.9$, for J/ψ and $\psi(2S)$ production in $p+p$ and $p+d$ interaction at 120 GeV. The error bars represent the total uncertainties. The curves correspond to fits using the Kaplan form described in the text.

ization $d\sigma/dp_T^2 = c\left(1 + p_T^2/p_0^2\right)^{-6}$ [43] and the results of the fits are shown in Fig. 5. The $\langle p_T\rangle$ and $\langle p_T^2\rangle$ can be expressed as

$$\langle p_T\rangle = \frac{35\pi p_0}{256}, \quad \langle p_T^2\rangle = \frac{p_0^2}{4}. \tag{3}$$

And the values of $\langle p_T^2\rangle$ are also listed in Table 2, showing very similar values for $p+p$ and $p+d$, as well as for J/ψ and $\psi(2S)$. While the p_T distributions cannot be reliably calculated for $p_T \ll M$ with fixed-order perturbative calculations, nonetheless, they could be calculated within the NRQCD framework by including the soft-gluon resummation, as outlined in Ref. [44]. It would be interesting to compare our results on the x_F and p_T dependence with NRQCD calculations including soft-gluon resummation.

The extracted $\langle p_T^2\rangle$ for $p+p \to J/\psi$ is compared with results from NA3 [31], NA51 [32], ISR [33] and PHENIX [34] in Fig. 6. The $\langle p_T^2\rangle$ increases logarithmically as $\sqrt{s}$ increases over a wide range of energies.

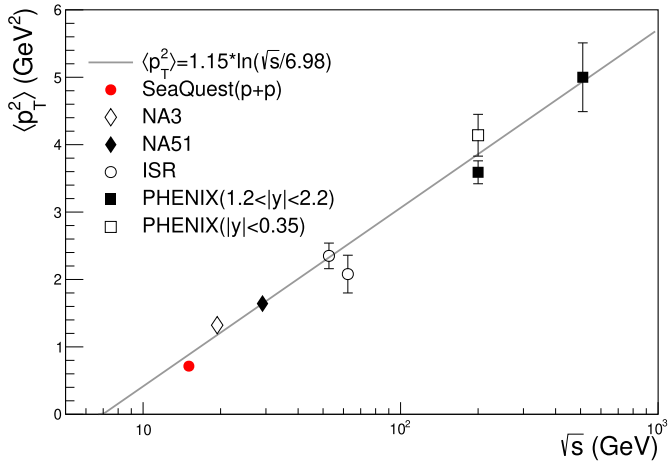

Fig. 6. The extracted $\langle p_T^2\rangle$ for $p+p \to J/\psi$ from SeaQuest (solid red circle) compared to other experiments [31–34] at different $\sqrt{s}$. The $\langle p_T^2\rangle$ increases logarithmically versus $\sqrt{s}$, as illustrated by the fit (gray line) to the data.

A linear fit versus the log of the center-of-mass energy, adapted from Ref. [34],

$$\langle p_T^2\rangle = a \ln\left(\sqrt{s}/b\right), \tag{4}$$

with

$$a = (1.150 \pm 0.043)\,\text{GeV}^2,\ b = (6.98 \pm 0.37)\,\text{GeV}, \tag{5}$$

describes the general trend. Some variation is expected due to the differing rapidity range of the measurements, as shown in previous fixed-target J/ψ production measurements [45].

The $\sigma_{pd}/2\sigma_{pp}$ J/ψ cross section ratios versus x_F are shown in Fig. 7. As a result of the identical target geometry of the two liquid targets and the frequent interchange between the targets, most of the systematic uncertainties largely cancel in the cross section ratio. The remaining systematic uncertainties shown in Fig. 7 have dominant contributions from the uncertainties associated with the mass-fitting procedure. Also shown in Fig. 7 is the J/ψ cross section ratio at $x_F \approx 0$ measured by the NA51 collaboration [19] with the 450 GeV proton beam. The average ratio for the J/ψ production across the SeaQuest measured region is $\approx 1.055 \pm 0.033 \pm 0.025$. Both the SeaQuest and the NA51 data show that the $\sigma_{pd}/2\sigma_{pp}$ ratios for J/ψ production are greater than unity with $\approx 2\sigma$ significance.

The $\sigma_{pd}/2\sigma_{pp}$ cross section ratio for J/ψ and $\psi(2S)$ production is also compared with the Drell-Yan process [4] in Fig. 7. The difference between the Drell-Yan and the charmonium cross section ratios in Fig. 7 clearly reflects the different underlying mechanisms in these two processes. The Drell-Yan process, dominated by the $q\bar{q}$ annihilation subprocess, leads to the expectation that the cross section ratio is

approximately $\left(1+\bar{d}(x_2)/\bar{u}(x_2)\right)/2$ at forward x_F [4], where x_2 is the momentum fraction of the parton in the target proton. The measured range of $0.5 < x_F < 0.9$ corresponds to $0.048 < x_2 < 0.078$ for J/ψ production, which covers a region of x_2 smaller than that covered by the Drell-Yan process ($0.13 < x_2 < 0.45$) [3,4]. For charmonium production, the gluon-gluon fusion subprocess alone would give a cross section ratio as $\left(1+g_n(x_2)/g_p(x_2)\right)/2$, where $g_{p,n}$ refers to the gluon distribution in the proton or neutron. As the gluon is an iso-scalar particle, one expects an identical charmonium production cross section per nucleon for $p+d$ and $p+p$. This prediction clearly would be modified once the contribution from the $q\bar{q}$ annihilation subprocess to the charmonium production is included. It should also be noted as the strong interaction is insensitive to the electric charge of the quarks, the relative weighting between $u\bar{u}$ and $d\bar{d}$ is different between charmonium production and the Drell-Yan process. As a result, the charmonium production is less sensitive to the light sea-quark asymmetry than the Drell-Yan process. The red solid curve in Fig. 7, obtained from the NRQCD calculation using the NNPDF4.0 proton PDFs, is in good agreement with the J/ψ cross section ratio data. The clear deviation from unity for the calculated ratio indicates a sizable contribution from the $q\bar{q}$ annihilation at the large x_F region, even though the gluon-gluon fusion remains important for J/ψ production at lower x_F. For comparison, the black dot-dashed curve in Fig. 7, corresponding to the NLO calculation for the Drell-Yan cross section ratio, gives significantly larger values for the ratio in qualitative agreement with the data. Our results are also compared with CEM calculations in Fig. S2 of the Supplemental Material.

In summary, the SeaQuest experiment has measured the cross sections for J/ψ and $\psi(2S)$ in $p+p$ and $p+d$ interactions at 120 GeV. The x_F dependence of the J/ψ and $\psi(2S)$ production cross sections is well described by the NRQCD calculation. The $\sigma_{\psi(2S)}/\sigma_{J/\psi}$ ratio is also shown. The measured ratio increases as x_F increases, indicating the increasing importance of $q\bar{q}$ annihilation in $\psi(2S)$ production. The p_T dependence is also reported. The extracted $\langle p_T^2 \rangle$ from this measurement follows an increasing pattern versus $\sqrt{s}$ established by data over a wide range of energies.

We also present a direct comparison of $\sigma_{pd}/2\sigma_{pp}$ between J/ψ production and the Drell-Yan process. While the Drell-Yan process proceeds via $q\bar{q}$ annihilation, J/ψ production has contributions from both the $q\bar{q}$ annihilation and the gg fusion processes. The measured $\sigma_{pd}/2\sigma_{pp}$ ratios are greater than unity for both the Drell-Yan and J/ψ production, showing that both processes are sensitive to the $\bar{d},\bar{u}$ flavor asymmetry of the proton sea. The smaller values of $\sigma_{pd}/2\sigma_{pp}$ for J/ψ production reflect the dilution due to the additional contribution of gg fusion for charmonium production. It would be interesting to include the $\sigma_{pd}/2\sigma_{pp}$ J/ψ data in a future extraction of the $\bar{d}/\bar{u}$ asymmetry of the proton.

Declaration of competing interest

The authors declare that they have no known competing financial interests or personal relationships that could have appeared to influence the work reported in this paper.

Data availability

Data will be made available on request.

Acknowledgements

We thank G. T. Garvey for contributions to the early stages of this experiment and M. Diefenthaler, L. Guo, B. Kerns, N. Kitts, N. C. R. Makins, I. Mooney, A. J. Puckett, D. Su, B. G. Tice, S. Watson, Z. Xi for their contributions to the execution of the experiment. We also thank the Fermilab Accelerator Division and Particle Physics Division for their support of this experiment. This work was performed by the SeaQuest Collaboration, whose work was supported in part by the US Department of Energy under Grant No. DE-AC02-06CH11357, No. DE-FG02-03ER41243, No. DE-FG02-07ER41528, and No. DE-FG02-94ER40847; the US National Science Foundation under Grants No. PHY 2013002, No. PHY 1812340, No. PHY 2110898, No. PHY 2110229, No. PHY 2111046, No. PHY 2209348, and No. PHY 2309922; National Science and Technology Council of Taiwan (R.O.C.); the JSPS (Japan) KAKENHI through Grants No. 21244028, No. 25247037, No. 25800133, No. 20K04000 and No. 22H01244. Fermilab is managed by Fermi Research Alliance, LLC (FRA), acting under Contract No. DE-AC02-07CH11359.

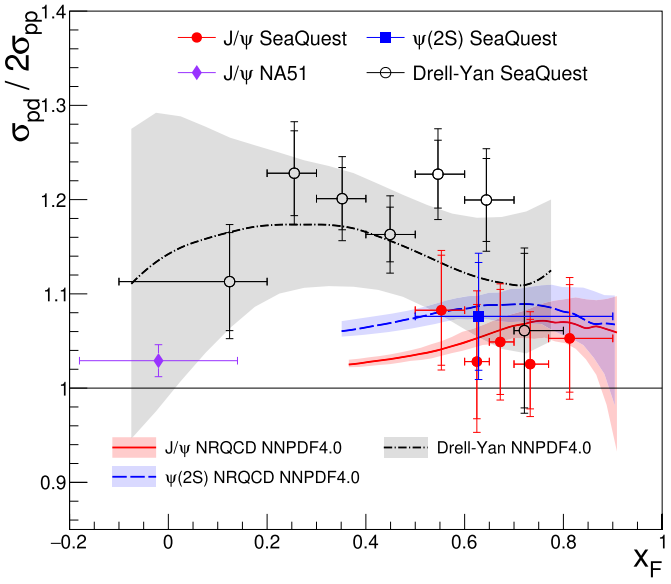

Fig. 7. The $\sigma_{pd}/2\sigma_{pp}$ cross section ratios for J/ψ (red circle) and $\psi(2S)$ (blue square) versus x_F from SeaQuest. The inner (outer) error bars represent the statistical (total) uncertainties. For comparison, the ratio for J/ψ measured by NA51 [19] and the ratios for the Drell-Yan cross sections by SeaQuest [4] are also shown. The solid (dashed) curve is the calculation for the J/ψ ($\psi(2S)$) cross section ratios at 120 GeV in the NRQCD model using the proton PDFs from NNPDF4.0 [23]. The dot-dashed curve represents the NLO Drell-Yan cross section ratios calculated with the same PDFs. The error bands indicate 68% confidence level from the PDFs.

Appendix A. Supplementary material

Supplementary material related to this article can be found online at https://doi.org/10.1016/j.physletb.2024.139032.

References

[1] C.A. Aidala, et al., The SeaQuest spectrometer at Fermilab, Nucl. Instrum. Methods Phys. Res., Sect. A 930 (2019) 49–63, https://doi.org/10.1016/j.nima.2019.03.039, arXiv:1706.09990.

[2] S.D. Drell, T.-M. Yan, Massive lepton-pair production in hadron-hadron collisions at high energies, Phys. Rev. Lett. 25 (5) (1970) 316–320, https://doi.org/10.1103/PhysRevLett.25.316 Erratum: Phys. Rev. Lett. 25 (1970) 902.

[3] J. Dove, et al., The asymmetry of antimatter in the proton, Nature 590 (7847) (2021) 561–565, https://doi.org/10.1038/s41586-021-03282-z; Publisher's correction: Nature 604 (2022) E26, arXiv:2103.04024.

[4] J. Dove, et al., Measurement of flavor asymmetry of light-quark sea in the proton with Drell-Yan dimuon production in $p+p$ and $p+d$ collisions at 120 GeV, Phys. Rev. C 108 (3) (2023) 035202, https://doi.org/10.1103/PhysRevC.108.035202, arXiv:2212.12160.

[5] J.C. Peng, D.M. Jansen, Y.C. Chen, Probing $\bar{u}/\bar{d}$ asymmetry in the proton via quarkonium production, Phys. Lett. B 344 (1) (1995) 1–5, https://doi.org/10.1016/0370-2693(94)01466-P, arXiv:hep-ph/9508244.

[6] G. Piller, A.W. Thomas, J/ψ production as a probe of charge symmetry violations and nuclear corrections in parton distributions, Z. Phys. C, Part. Fields 70 (4) (1996) 661–664, https://doi.org/10.1007/s002880050140, arXiv:hep-ph/9508410.

[7] E.J. Stephenson, et al., Observation of the charge symmetry breaking $d+d \rightarrow {}^4\mathrm{He}+\pi^0$ reaction near threshold, Phys. Rev. Lett. 91 (14) (2003) 142302, https://doi.org/10.1103/PhysRevLett.91.142302, arXiv:nucl-ex/0305032.

[8] A.K. Opper, et al., Charge symmetry breaking in $np \to d\pi^0$, Phys. Rev. Lett. 91 (21) (2003) 212302, https://doi.org/10.1103/PhysRevLett.91.212302, arXiv:nucl-ex/0306027.

[9] J.T. Londergan, J.C. Peng, A.W. Thomas, Charge symmetry at the partonic level, Rev. Mod. Phys. 82 (3) (2010) 2009–2052, https://doi.org/10.1103/RevModPhys.82.2009, arXiv:0907.2352.

[10] L.Y. Zhu, et al., Measurement of Υ production for $p+p$ and $p+d$ interactions at 800 GeV/c, Phys. Rev. Lett. 100 (6) (2008) 062301, https://doi.org/10.1103/PhysRevLett.100.062301, arXiv:0710.2344.

[11] J.P. Lansberg, et al., Quarkonium physics at a fixed-target experiment using the LHC beams, Few-Body Syst. 53 (1) (2012) 11–25, https://doi.org/10.1007/s00601-012-0445-8, arXiv:1204.5793.

[12] R. Vogt, J/ψ production and suppression, Phys. Rep. 310 (4) (1999) 197–260, https://doi.org/10.1016/S0370-1573(98)00074-X.

[13] M.B. Einhorn, S.D. Ellis, Hadronic production of the new resonances: probing gluon distributions, Phys. Rev. D 12 (7) (1975) 2007–2014, https://doi.org/10.1103/PhysRevD.12.2007.

[14] H. Fritzsch, Producing heavy quark flavors in hadronic collisions— a test of quantum chromodynamics, Phys. Lett. B 67 (2) (1977) 217–221, https://doi.org/10.1016/0370-2693(77)90108-3.

[15] F. Halzen, CVC for gluons and hadroproduction of quark flavours, Phys. Lett. B 69 (1) (1977) 105–108, https://doi.org/10.1016/0370-2693(77)90144-7.

[16] C.-H. Chang, Hadronic production of J/ψ associated with a gluon, Nucl. Phys. B 172 (1980) 425–434, https://doi.org/10.1016/0550-3213(80)90175-3.

[17] G.T. Bodwin, E. Braaten, G.P. Lepage, Rigorous QCD analysis of inclusive annihilation and production of heavy quarkonium, Phys. Rev. D 51 (1995) 1125–1171, https://doi.org/10.1103/PhysRevD.55.5853 (ANL-HEP-PR-94-24, FERMILAB-PUB-94-073-T, NUHEP-TH-94-5); Erratum: Phys. Rev. D 55 (1997) 5853, https://doi.org/10.1103/PhysRevD.51.1125, arXiv:hep-ph/9407339.

[18] R. Vogt, x_F dependence of ψ and Drell-Yan production, Phys. Rev. C 61 (3) (2000) 035203, https://doi.org/10.1103/PhysRevC.61.035203, arXiv:hep-ph/9907317.

[19] M.C. Abreu, et al., J/ψ, ψ' and Drell-Yan production in pp and pd interactions at 450 GeV/c, Phys. Lett. B 438 (1) (1998) 35–40, https://doi.org/10.1016/S0370-2693(98)01014-4.

[20] M. Beneke, I.Z. Rothstein, Hadroproduction of quarkonium in fixed-target experiments, Phys. Rev. D 54 (3) (1996) 2005, https://doi.org/10.1103/PhysRevD.54.2005; Erratum: Phys. Rev. D 54 (1996) 7082, arXiv:hep-ph/9603400.

[21] W.-C. Chang, et al., Fixed-target charmonium production and pion parton distributions, Phys. Rev. D 107 (5) (2023) 056008, https://doi.org/10.1103/PhysRevD.107.056008, arXiv:2209.04072.

[22] T.-J. Hou, et al., New CTEQ global analysis of quantum chromodynamics with high-precision data from the LHC, Phys. Rev. D 103 (1) (2021) 014013, https://doi.org/10.1103/PhysRevD.103.014013, arXiv:1912.10053.

[23] R.D. Ball, et al., The path to proton structure at 1% accuracy, Eur. Phys. J. C 82 (2022) 428, https://doi.org/10.1140/epjc/s10052-022-10328-7 (Edinburgh 2021/12, Nikhef-2021-013, TIF-UNIMI-2021-11), arXiv:2109.02653.

[24] S. Agostinelli, et al., GEANT4—a simulation toolkit, Nucl. Instrum. Methods A 506 (3) (2003) 250–303, https://doi.org/10.1016/S0168-9002(03)01368-8.

[25] J. Allison, et al., GEANT4 developments and applications, IEEE Trans. Nucl. Sci. 53 (1) (2006) 270, https://doi.org/10.1109/TNS.2006.869826.

[26] J. Allison, et al., Recent developments in GEANT4, Nucl. Instrum. Methods Phys. Res., Sect. A 835 (2016) 186–225, https://doi.org/10.1016/j.nima.2016.06.125.

[27] S. Catani, et al., Vector boson production at hadron colliders: a fully exclusive QCD calculation at next-to-next-to-leading order, Phys. Rev. Lett. 103 (8) (2009) 082001, https://doi.org/10.1103/PhysRevLett.103.082001, arXiv:0903.2120.

[28] S. Dulat, et al., New parton distribution functions from a global analysis of quantum chromodynamics, Phys. Rev. D 93 (3) (2016) 033006, https://doi.org/10.1103/PhysRevD.93.033006, arXiv:1506.07443.

[29] S.F. Pate, et al., Estimation of combinatoric background in seaquest using an event-mixing method, J. Instrum. 18 (10) (2023) P10032, https://doi.org/10.1088/1748-0221/18/10/P10032, arXiv:2302.04152.

[30] R.L. Workman, et al., Review of particle physics, Prog. Theor. Exp. Phys. 2022 (8) (2022) 083C01, https://doi.org/10.1093/ptep/ptac097.

[31] J. Badier, et al., Experimental J/ψ hadronic production from 150 to 280 GeV/c, Z. Phys. C, Part. Fields 20 (1983) 101–116, https://doi.org/10.1007/BF01573213 (CERN-EP/83-86).

[32] O. Drapier, Étude des distributions en impulsion transverse des dimuons produits dans les collisions noyau-noyau auprès du SPS du CERN, Ph.D. thesis, Lyon 1, 1998, https://cds.cern.ch/record/461496.

[33] A. Clark, et al., Electron pair production at the CERN ISR, Nucl. Phys. B 142 (1) (1978) 29–52, https://doi.org/10.1016/0550-3213(78)90400-5.

[34] U.A. Acharya, et al., J/ψ and $\psi(2s)$ production at forward rapidity in $p+p$ collisions at $\sqrt{s} = 510$ GeV, Phys. Rev. D 101 (5) (2020) 052006, https://doi.org/10.1103/PhysRevD.101.052006, arXiv:1912.13424.

[35] C.H. Leung, Probing parton distributions in proton using Drell-Yan and charmonium production in $p+p$ and $p+d$ interactions with 120 GeV proton beam at Fermilab, Ph.D. thesis, University of Illinois at Urbana-Champaign, 2024, https://hdl.handle.net/2142/124206.

[36] F. Maltoni, et al., Analysis of charmonium production at fixed-target experiments in the NRQCD approach, Phys. Lett. B 638 (2) (2006) 202–208, https://doi.org/10.1016/j.physletb.2006.05.010, arXiv:hep-ph/0601203.

[37] P. Nason, S. Dawson, R.K. Ellis, The total cross section for the production of heavy quarks in hadronic collisions, Nucl. Phys. B 303 (4) (1988) 607–633, https://doi.org/10.1016/0550-3213(88)90422-1.

[38] P. Nason, S. Dawson, R.K. Ellis, The one particle inclusive differential cross section for heavy quark production in hadronic collisions, Nucl. Phys. B 327 (1) (1989) 49–92, https://doi.org/10.1016/0550-3213(89)90286-1; Erratum: Nucl. Phys. B 335 (1990) 260.

[39] M.L. Mangano, P. Nason, G. Ridolfi, Fixed-target hadroproduction of heavy quarks, Nucl. Phys. B 405 (2) (1993) 507–535, https://doi.org/10.1016/0550-3213(93)90557-6.

[40] G.A. Schuler, R. Vogt, Systematics of quarkonium production, Phys. Lett. B 387 (1) (1996) 181–186, https://doi.org/10.1016/0370-2693(96)00999-9, arXiv:hep-ph/9606410.

[41] R.E. Nelson, R. Vogt, A.D. Frawley, Narrowing the uncertainty on the total charm cross section and its effect on the J/ψ cross section, Phys. Rev. C 87 (1) (2013) 014908, https://doi.org/10.1103/PhysRevC.87.014908, arXiv:1210.4610.

[42] J.G. Heinrich, et al., Higher-twist effects in the reaction $\pi^- N \to \mu^+\mu^- X$ at 253 GeV/c, Phys. Rev. D 44 (7) (1991) 1909–1932, https://doi.org/10.1103/PhysRevD.44.1909.

[43] D.M. Kaplan, et al., Study of the high-mass dimuon continuum in 400-GeV proton-nucleus collisions, Phys. Rev. Lett. 40 (7) (1978) 435–438, https://doi.org/10.1103/PhysRevLett.40.435.

[44] P. Sun, C.-P. Yuan, F. Yuan, Heavy quarkonium production at low $P_\perp$ in nonrelativistic QCD with soft gluon resummation, Phys. Rev. D 88 (5) (2013) 054008, https://doi.org/10.1103/PhysRevD.88.054008, arXiv:1210.3432.

[45] C. Biino, et al., J/ψ longitudinal polarization from πN interactions, Phys. Rev. Lett. 58 (24) (1987) 2523–2526, https://doi.org/10.1103/PhysRevLett.58.2523.